Uncertainty Analysis to C5G7-TD Benchmark Based on the COST Method

Liangzhi Cao*, Zhuojie Sui, Bo Wang, Chenghui Wan, Zhouyu Liu
School of Nuclear Science and Technology, Xi'an Jiaotong University, Xi'an, Shaanxi, China
caolz@mail.xjtu.edu.cn

ABSTRACT

A method of Covariance-Oriented Sample Transformation (COST) has been proposed in our previous work to provide the converged uncertainty analysis results with a minimal sample size. The transient calculation of nuclear reactor is a key part of the reactor-physics simulation, so the accuracy and confidence of the neutron kinetics results have attracted much attention. In this paper, the Uncertainty Quantification (UQ) function of the high fidelity neutronics code NECP-X has been developed based on our home-developed uncertainty analysis code UNICORN, building a platform for the UQ of the transient calculation. Furthermore, the well-known space-time heterogeneous neutron kinetics benchmark C5G7 and its uncertainty propagation from the nuclear data to the interested key parameters of the core have been investigated. To address the problem of "the curse of dimensionality" caused by the large number of input parameters, the COST method has been applied to generate multivariate normal-distribution samples in uncertainty analysis. As a result, the law of the assembly/pin normalized power and their uncertainty with respect to time after introducing an instantaneous perturbation has been obtained. From the numerical results, it can be observed that the maximum relative uncertainties for the assembly normalized power can up to be about 1.65% and the value for the pin-wise power distributions can be about 2.71%.

KEYWORDS: Uncertainty analysis, Covariance-Oriented Sample Transformation, C5G7 benchmark problem, transient modeling and simulation

1. INTRODUCTION

With the great efforts made by OECD/NEA, a series of space-time neutron kinetics benchmark problems have been proposed [1]. These benchmark problems are based on the well-studied steady-state C5G7 benchmark. The transient analysis towards the C5G7 benchmark problem has been focused on after the proposal of the benchmark [2-4]. And the recent transient-analysis results towards C5G7 benchmark problems have been summarized by Hou J. at the 2019 workshop [5]. All the researches towards the C5G7 transient benchmark are focused on the transient modeling and simulations, no researches have performed the uncertainty analysis, which is the next-step objective of this benchmark. Therefore, the uncertainty analysis has been focused on in this paper, aimed at propagating the nuclear-data uncertainties to the interested key parameters of the transient modeling and simulations for the C5G7 transient benchmark.

The methods of uncertainty analysis can be divided into two categories: the deterministic methods and the statistical sampling methods. Compared with the deterministic method, the statistical sampling method can provide the uncertainty analysis results without any low-order approximation and is universally applicable to all kinds of systems. Therefore, it is regarded as the appropriate methodology to perform the uncertainty analysis for the transient modeling and simulations. However, due to the multiple dimensions of the input parameters in the transient calculation, the statistical sampling methods face the problem of

"the curse of dimensionality". In order to fully describe the probability distribution of the input parameters, the sample size required by the conventional sampling methods is very huge, resulting in corresponding computational challenge. The COST method has been proposed in our previous work to provide the converged UQ results with a minimal sample size [6].

In this context, the uncertainty analysis has been implemented to the transient modeling and simulations of the C5G7 benchmark problem based on the COST method, quantifying the uncertainties of the interested key parameters during the transient process due to the nuclear-data uncertainties. As the numerical results, the relative uncertainties of the assembly normalized power and also pin-wise power distributions have been quantified during the transient process.

2. THE IMPLEMENTATION OF THE COST METHOD

The COST method can directionally "hand-pick" a small sample ensemble so that the calculation of a very-huge sample can be replaced by a single calculation of a very small sample. Furthermore, the covariance matrix of the COST samples can fully map back to the target covariance matrix of the given population. This means the samples can carry all the information of the target covariance matrix which describes the uncertainty of input parameters. Meanwhile, the minimum sample size required by COST can be determined in advance based on the current input-parameter covariance matrix, which is lower than the dimension of the input parameters.

The implementation of the COST method includes the following steps. Firstly, like the first step of the conventional sampling method, the uncertainties of cross sections can be characterized by the group-wise covariance matrix. Based on the covariance information of the nuclear data in the evaluation nuclear database, the relative input-parameter covariance matrix $\boldsymbol{\Sigma}$ of the considered multi-group cross-section characterized can be constructed. Therefore, the joint probability density function of the input parameters is determined as follows:

$$g(\boldsymbol{X}) = \frac{1}{2\boldsymbol{\pi}^{NV/2}\sqrt{|\boldsymbol{\Sigma}|}} exp\left(-\frac{1}{2}(\boldsymbol{X}-\boldsymbol{\mu})^{T}\boldsymbol{\Sigma}^{-1}(\boldsymbol{X}-\boldsymbol{\mu})\right) \tag{1}$$

where $\boldsymbol{X} = [\sigma_1,\sigma_2,\ldots,\sigma_{NV}]^{\mathrm{T}}$, represents the input parameter vectors consisting of multi-group cross sections of all nuclides, reaction channels and energy groups that need to be analyzed, in which NV is the dimension of it; $\boldsymbol{\mu}$ is the mean vector of the input parameter. Then the eigenvalue decomposition of the matrix is used to diagonalize $\boldsymbol{\Sigma}$:

$$\boldsymbol{\Sigma} = \boldsymbol{U}\boldsymbol{\Lambda}_{\boldsymbol{\Sigma}}\boldsymbol{U}^{T} \tag{2}$$

The eigenvalues and corresponding eigenvectors are arranged in descending order. The number of non-zero eigenvalues, i.e. the rank of $\boldsymbol{\Sigma}$ is counted which can be denoted by r, and here, r is the minimum sample sizes required for convergence.

Secondly, given standard normal distribution population with the dimension equaling NV, which can be donated as $\boldsymbol{N}_{NV}(\boldsymbol{0}, \boldsymbol{I})$. Given any sample size NS not less than r, the standard normal distribution $\boldsymbol{Z} \sim \boldsymbol{N}_{NV}(\boldsymbol{0}, \boldsymbol{I})$ ($\boldsymbol{I}$ is a unit matrix) is sampled by user-specified sampling technique (Latin Hypercube Sampling technique in this paper) to generate sample space characterized as $\boldsymbol{Z}_{\boldsymbol{S}}$. It should be noted that the sample size should be big enough to fully describe the one-dimensional standard normal distribution when r is too small. In the calculation of subsequent chapters, the sample size is set to 30 under such a situation. Then, calculate the sample covariance matrix of $\boldsymbol{Z}_{\boldsymbol{S}}$ which can be characterized as $\boldsymbol{I}^{*}$, and the eigenvalue decomposition of the matrix is used to diagonalize $\boldsymbol{I}^{*}$.

$$\boldsymbol{I}^{*} = \boldsymbol{P}\boldsymbol{\Lambda}_{\boldsymbol{I}^{*}}\boldsymbol{P}^{T} \tag{3}$$

The eigenvalues and corresponding eigenvectors are arranged in descending order. The number of non-zero eigenvalues, i.e. the rank of $\boldsymbol{I}^*$ is counted and can be denoted by k. Note that there is a condition $k \geq r$ that needs to be satisfied. If $k<r$, repeat this step to reproduce $\boldsymbol{Z_S}$ until the condition is met.

Thirdly, matrix $\boldsymbol{L}$ and matrix $\boldsymbol{R}$ are determined by the following formula：

$$\boldsymbol{L} = \boldsymbol{P}_k \boldsymbol{\Lambda}_{I^*k}^{1/2} \ ; \boldsymbol{R} = \boldsymbol{U}_k \boldsymbol{\Lambda}_{\Sigma k}^{1/2} \tag{4}$$

Where $\boldsymbol{U_k}$ and $\boldsymbol{P_k}$ is $NV \times k$ and represents the matrix composed of the first k eigenvectors of $\boldsymbol{\Sigma}$ and $\boldsymbol{I}^*$ corresponding to eigenvalue order respectively; $\boldsymbol{\Lambda_{\Sigma k}}$ and $\boldsymbol{\Lambda_{I^*k}}$ is $k \times k$, representing the diagonal matrix composed of the first k eigenvalues of $\boldsymbol{\Sigma}$ and $\boldsymbol{I}^*$ arranged in descending order respectively.

$$\boldsymbol{U}_k = \left(\boldsymbol{u}_{\Sigma 1}, \boldsymbol{u}_{\Sigma 2}, \ldots, \boldsymbol{u}_{\Sigma k}\right); \boldsymbol{\Lambda}_{\Sigma k} = \begin{pmatrix} \overbrace{\begin{matrix} \ell_{\Sigma 1} & & \\ & \ddots & \\ & & \lambda_{\Sigma r} \end{matrix}}^{k} & \boldsymbol{0} \\ \boldsymbol{0} & 0 \end{pmatrix}; \boldsymbol{P}_k = \left(\boldsymbol{p}_{I^* 1}, \boldsymbol{p}_{I^* 2}, \ldots, \boldsymbol{p}_{I^* k}\right); \boldsymbol{\Lambda}_{I^* k} = \begin{pmatrix} \lambda_{I^* 1} & & \boldsymbol{0} \\ & \ddots & \\ \boldsymbol{0} & & \lambda_{I^* k} \end{pmatrix} \tag{5}$$

Then find an invertible matrix $\boldsymbol{F}$ by Eq.(6), which can transform $\boldsymbol{L}$ into the row simplest matrix.

$$\boldsymbol{F}\left(\boldsymbol{L} \mid \boldsymbol{I}_{NV}\right) \overset{r}{\square} \left(\begin{array}{c|c} \boldsymbol{I}_k & \\ \hline \boldsymbol{O} & \boldsymbol{F} \end{array}\right) \tag{6}$$

where $\boldsymbol{I_k}$ is $k \times k$, represents the matrix consisting of non-zero rows (total of k rows) in the row simplest matrix of $\boldsymbol{L}$, that is, the k-dimensional unit matrix. $\boldsymbol{I_{NV}}$ is $NV \times NV$, represents the NV-dimensional unit matrix. Meanwhile, a square matrix $\boldsymbol{S}$ of $NV \times NV$ is constructed based on Eq.(7), whose order is equal to the dimension of the input parameter:

$$\boldsymbol{S} = \left(\boldsymbol{R} \mid \boldsymbol{O}\right) \tag{7}$$

Finally, based on matrix $\boldsymbol{S}$ and $\boldsymbol{F}$, the transformation matrix $\boldsymbol{A}$ can be obtained by Eq.(8) for linear transformation.

$$\boldsymbol{A} = \boldsymbol{SF} \tag{8}$$

Like the last step of the conventional sampling method, samples $\boldsymbol{X_S}$ are generated using Eq.(9) to propagate the input parameter uncertainties completely.

$$\boldsymbol{X}_S = \boldsymbol{A}\boldsymbol{Z}_S + \boldsymbol{V}; \quad \boldsymbol{V} = \left[\overbrace{\boldsymbol{\mu}, \boldsymbol{\mu}, \ldots, \boldsymbol{\mu}}^{NS}\right] \tag{9}$$

where $\boldsymbol{X_S}$ is a sample set of the input parameter $\boldsymbol{X}$;. $\boldsymbol{X_S}$ and $\boldsymbol{Z_S}$ have the same dimension $NV \times NS$. $\boldsymbol{A}$ is the transformation matrix with the dimension of $NV \times NV$. $\boldsymbol{V}$ represents the extended matrix of $\boldsymbol{\mu}$ with the dimension of $NV \times NS$. Then the next step of uncertainty analysis based on the sampling method will be continued.

3. NUMERICAL RESULTS AND ANALYSIS

The COST method has been integrated in our home-developed uncertainty analysis code named UNICORN [7] to provide multivariate samples. In this section, the nuclear-data uncertainties are generally characterized by the multigroup cross-section covariance libraries, which were generated by NJOY [8] based on ENDF/B-VII.1. Moreover, our home-developed high-fidelity PWR code named as NECP-X [9] was used for the transient modeling and simulation for the C5G7 benchmark. As both the multigroup microscopic cross-section library and continue-energy cross-section library were required in NECP-X for the modeling and simulation, hence the continue-energy cross-section perturbation model

has been established in UNICORN to generate the cross-section samples based on the corresponding covariance libraries. Based on all above, the nuclear-data uncertainties have been propagated to the interested key parameters during the transient process for the C5G7 benchmark problem. As the numerical results, the relative uncertainties of the assembly normalized power and also pin-wise power distributions have been quantified during the transient process.

3.1 Calculating Conditions and Parameter Settings

Based on the C5G7 essential information about the geometry information for the pin-cells and assemblies and isotopic concentrations for all the loaded materials, the NECP-X code is applied to execute the modeling and simulation for the transient exercise of C5G7 benchmark from the microscopic cross-section library. The transient exercise is the process to insert and then withdraw the bank 1, which is at the position of the UO2-loaded fuel assembly in middle of the core. At beginning, the TD0-1 exercise proposed in C5G7 transient benchmark has been selected and tested. However, it was observed that the negative reactivity was huge (about 16$) and the fuel-assembly power would decrease to be zero in very short time. Therefore, an appropriate insertion fraction (about 1%) has been determined to be applied for the transient modeling and simulation. As shown in Fig.1, in the transient exercise, the bank 1 is inserted with the insertion fraction of 1% at the initial time t=0.0s and the position of bank 1 is hold until the time t=1.0s; at time t=1.0s, the bank 1 is withdraw out of the core.

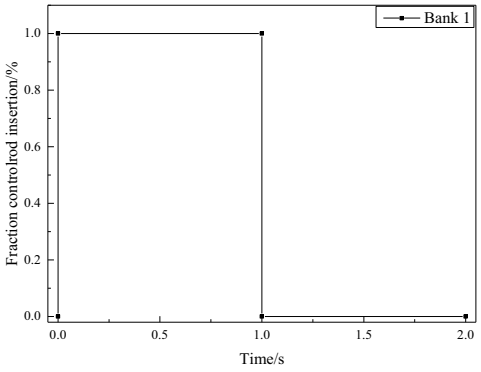

Figure 1. Control rod movement in the transient exercise

In this paper, the 2D model has been applied to perform the transient simulation for the transient exercise. And during the transient process, the thermal-hydraulics feedback is not considered, and the temperatures of the fuel and moderator remain at the hot conditions with the room temperature. Therefore, two different steady states have been modeled and simulated to determine the reactivity introduced in the core with the insertion of bank 1, including the state that the bank 1 out of the core and inserted with the insertion fraction of 1%. The k_{eff} of these two steady states and corresponding reactivity introduced by the bank insertion can be determined, as shown in Table I.

Table I. The k_{eff} and reactivity introduced by bank-1 insertion of C5G7

k_{eff} with bank-1 withdraw	k_{eff} with bank-1 insertion	Reactivity introduced
1.202867	1.146980	-4050.8pcm

Applying the NECP-X code, the transient process has been modeled and simulated. The time step is set to be 0.05s/step within 0.0s~2.0s and 0.1s/step within 2.0s~3.0s. The multi-group cross-section covariance library contains the uncertainty and correlation information and was generated based on ENDF/B-VII.1 using the NJOY code. For the uncertainty quantification, the UNICORN code has been applied using the COST method. The analyzed isotopes and corresponding cross sections as well as the

dimension of each isotope and the minimum sample size required by COST to generate samples for each isotope are also listed in Table II. It should be noted that the covariance information between nuclides is not given in the nuclear data libraries. So, in current studies, nuclides are considered to be independent with each other. If the dependence between nuclides is strictly considered, the number of computations required by COST will be 2276, and it is a big challenge for the computing resources. Therefore, this paper ignored the correlation between nuclides, and set the samples size to 262, which is the biggest one among all the nuclides.

Table II. The isotopes and corresponding cross sections in uncertainty analysis

Isotopes	Cross sections	Dimension *(NV)*	Sample size require by COST
^{235}U	$\sigma_{(n,elas)}$, $\sigma_{(n,inel)}$, $\sigma_{(n,2n)}$, $\sigma_{(n,f)}$, $\sigma_{(n,\gamma)}$, ν	414	258
^{238}U	$\sigma_{(n,elas)}$, $\sigma_{(n,inel)}$, $\sigma_{(n,2n)}$, $\sigma_{(n,f)}$, $\sigma_{(n,\gamma)}$, ν	414	262
^{238}Pu	$\sigma_{(n,elas)}$, $\sigma_{(n,inel)}$, $\sigma_{(n,2n)}$, $\sigma_{(n,f)}$, $\sigma_{(n,\gamma)}$	345	187
^{239}Pu	$\sigma_{(n,elas)}$, $\sigma_{(n,inel)}$, $\sigma_{(n,2n)}$, $\sigma_{(n,f)}$, $\sigma_{(n,\gamma)}$	345	214
^{240}Pu	$\sigma_{(n,elas)}$, $\sigma_{(n,inel)}$, $\sigma_{(n,2n)}$, $\sigma_{(n,f)}$, $\sigma_{(n,\gamma)}$	345	216
^{241}Pu	$\sigma_{(n,elas)}$, $\sigma_{(n,inel)}$, $\sigma_{(n,2n)}$, $\sigma_{(n,f)}$, $\sigma_{(n,\gamma)}$	345	153
^{242}Pu	$\sigma_{(n,elas)}$, $\sigma_{(n,inel)}$, $\sigma_{(n,2n)}$, $\sigma_{(n,f)}$, $\sigma_{(n,\gamma)}$	345	143
^{241}Am	$\sigma_{(n,elas)}$, $\sigma_{(n,inel)}$, $\sigma_{(n,2n)}$, $\sigma_{(n,f)}$, $\sigma_{(n,\gamma)}$	345	214
^{16}O	$\sigma_{(n,elas)}$, $\sigma_{(n,inel)}$, $\sigma_{(n,\gamma)}$, $\sigma_{(n,\alpha)}$	276	103
^{1}H	$\sigma_{(n,elas)}$, $\sigma_{(n,\gamma)}$	138	70
^{90}Zr	$\sigma_{(n,elas)}$, $\sigma_{(n,inel)}$, $\sigma_{(n,\gamma)}$	207	92
^{91}Zr	$\sigma_{(n,elas)}$, $\sigma_{(n,inel)}$, $\sigma_{(n,2n)}$, $\sigma_{(n,\gamma)}$	276	89
^{92}Zr	$\sigma_{(n,elas)}$, $\sigma_{(n,inel)}$, $\sigma_{(n,2n)}$, $\sigma_{(n,\gamma)}$	276	92
^{94}Zr	$\sigma_{(n,elas)}$, $\sigma_{(n,inel)}$, $\sigma_{(n,2n)}$, $\sigma_{(n,\gamma)}$	276	87
^{109}Ag	$\sigma_{(n,elas)}$, $\sigma_{(n,inel)}$, $\sigma_{(n,2n)}$, $\sigma_{(n,\gamma)}$	276	96
Total	---	4623	2276 // 262

3.2 Results for the Transient Uncertainty Analysis

As the numerical results for the uncertainty analysis, the interested fuel-assembly and pin-wise power distributions have been focused on and corresponding uncertainties have been quantified. The uncertainty results for the normalized fuel-assembly power are shown in Fig.2 and Fig.3. From the numerical results, several observations can be found. First, for the fuel assembly inserted with bank 1, the relative uncertainty of the normalized assembly power decreases with the time after the bank insertion; then after the bank withdraw, the relative uncertainty increases immediately and then increases very slowly with the time; combining the absolute uncertainty curve, it can be found that in the transient process, the absolute uncertainty has the same trend but with a larger range, so the change of relative uncertainty is mainly due to the change of the absolute uncertainty. Second, for the others fuel assemblies without bank 1 inserted, the relative uncertainties of the normalized assembly powers increase with the time after the bank insertion; then after the bank withdraw, the relative uncertainties decrease immediately and then decrease very slowly with the time; combining the absolute uncertainty curve, it can be found that in the transient process, the absolute uncertainty only changes slightly, so the change of relative uncertainty is mainly due to the influence of power change. These observed phenomenon are very interesting.

In order to explain the observed phenomenon mentioned above, the pin-wise power distributions have been focused on. The relative uncertainties of the pin-wise powers at t=0.0s, 0.05s, 1.0s and 1.05s are respectively shown in Fig.4. Through the observations of the pin-wise power distributions, the following observations can be provided. Before the bank 1 insertion, the pin-wise powers at #1 fuel assembly are the largest ones and those in #4 fuel assembly are the smallest. After the bank 1 inserted at the time t=0.05s, all the pin-wise powers decrease and also the fuel-assembly powers. By comparing the power distributions between t=0.0s and t=0.05s, the power of #1 assembly decreases from 0.48 to 0.32, with the

decreased ratio is about 33.3%; while for the others fuel assemblies, the decreased ratios are respectively 31.4% for #2 and #3 assembly and 30.6% for #4 assembly. Through the assembly-power normalization, the relative powers for #2, #3 and #4 assemblies have been raised by the larger power decrease in #1 assembly. In this case, the relative contributions of the fission cross sections to the fuel-assembly powers in #2, #3 and #4 fuel assemblies becomes larger after the bank 1 insertion. Therefore, after the bank 1 insertion, the relative uncertainties of the fuel-assembly power for #2, #3 and #4 assemblies increases lightly while #1 decreases lightly with the time. The process above becomes opposite after the bank 1 withdraw when t=1.0s and t=1.05s. When the bank 1 withdraw out of the core, the fuel-assembly power for #1 assembly increases immediately and becomes dominant, hence the relative contribution of the fission cross sections for #1 assembly becomes dominant and the relative uncertainty of the power in #1 assembly increases after bank 1 withdraw.

From the numerical values, for the transient process defined in this paper, the uncertainty-analysis results can be concluded as following. The maximum relative uncertainty for the normalized assembly powers can be about 1.65% and the minimum value is about 0.46%. For the pin-wise power distributions, the maximum relative uncertainty is about 2.71%.

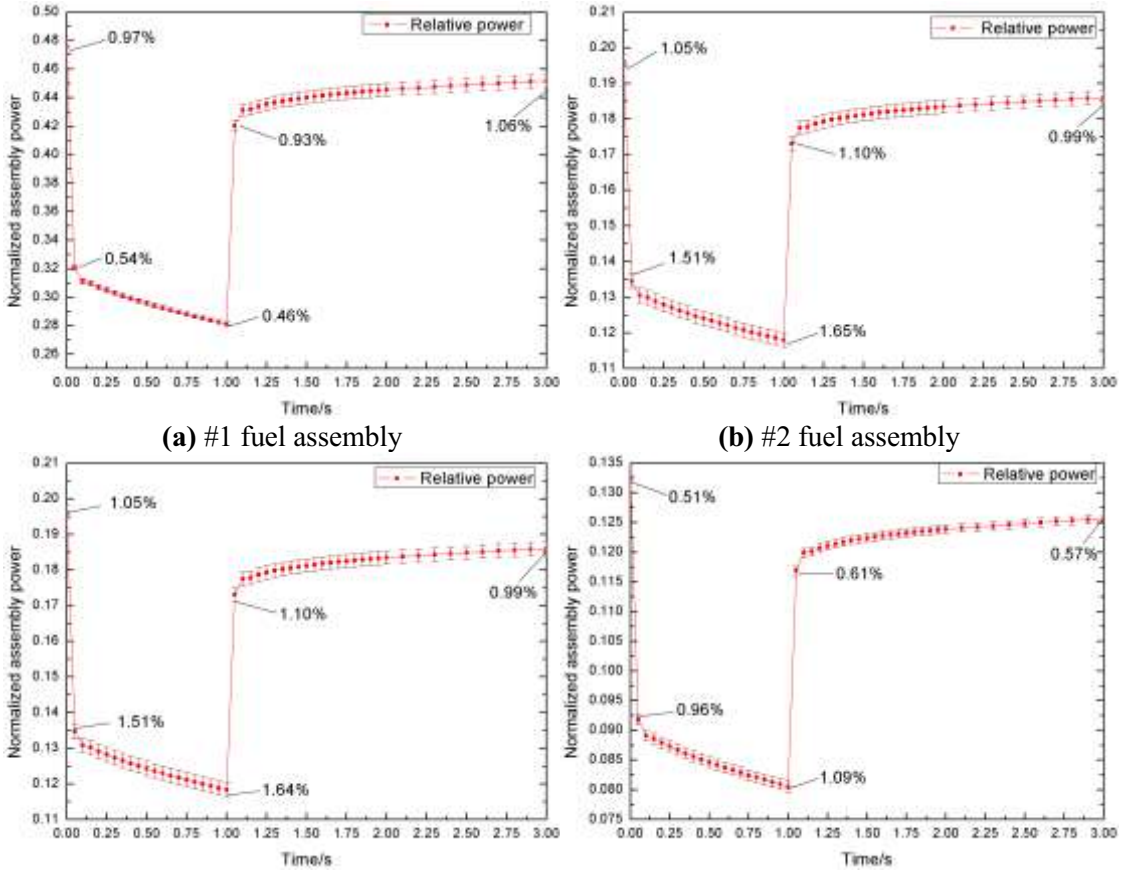

(a) #1 fuel assembly **(b)** #2 fuel assembly

(c) #3 fuel assembly **(d)** #4 fuel assembly

Figure 2. Normalized assembly powers and corresponding uncertainties

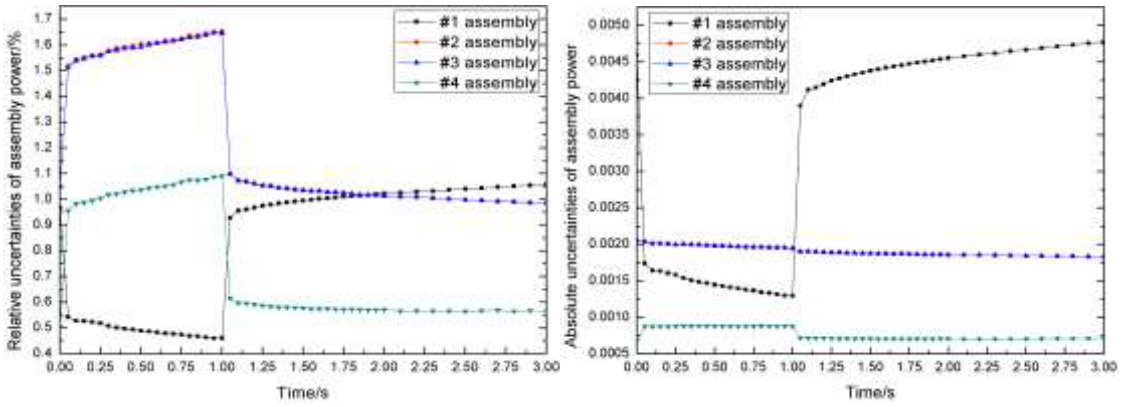

(a) Relative uncertainty **(b)** Absolute uncertainty

Figure 3. Uncertainty of the normalized fuel-assembly powers

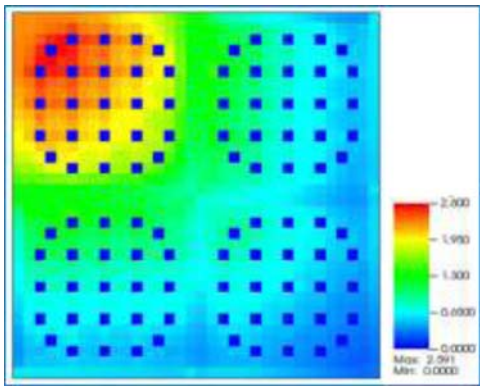

(a) pin-wise powers, t=0.0s

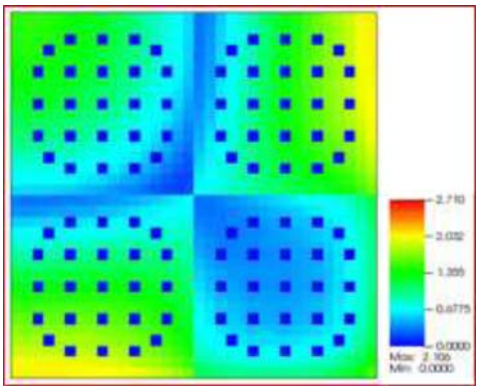

(b) relative uncertainties/%, t=0.0s

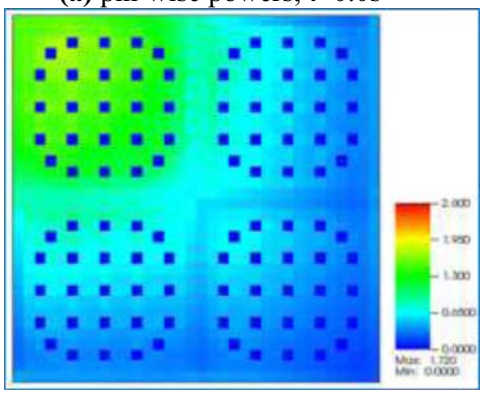

(c) pin-wise powers, t=0.05s

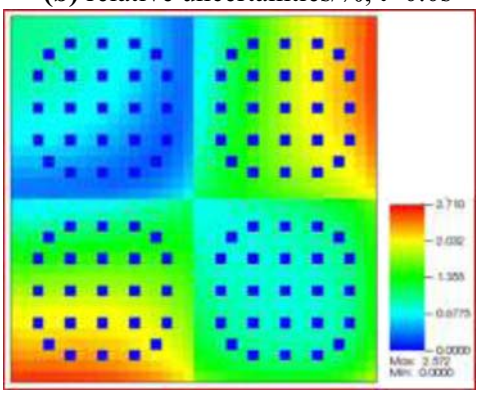

(d) relative uncertainties/%, t=0.05s

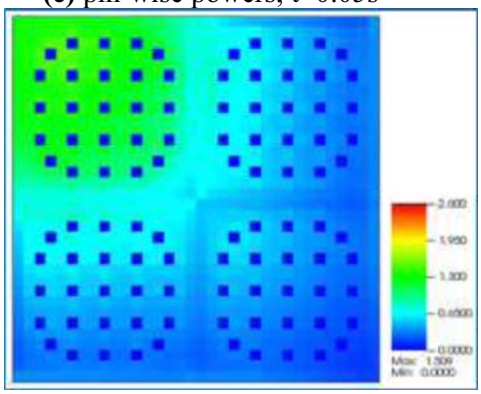

(e) pin-wise powers, t=1.0s

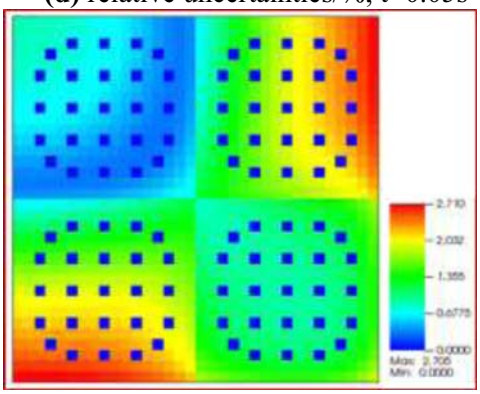

(f) relative uncertainties/%, t=1.0s

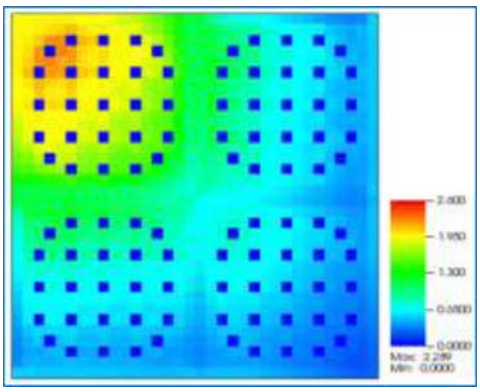

(g) pin-wise powers, t=1.05s

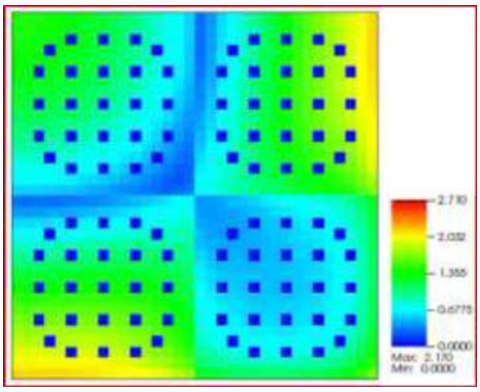

(h) relative uncertainties/%, t=1.05s

Figure 4. The pin-wise powers and corresponding relative uncertainties/%

4. CONCLUSIONS

In this paper, the COST method has been integrated in our home-developed uncertainty analysis code named UNICORN to provide better multivariate samples, propagating the nuclear-data uncertainties to the key parameters of the transient modeling and simulations. Then the uncertainty analysis has been performed to the C5G7 transient process from the microscopic cross-section library based on our home-developed high-fidelity PWR code NECP-X and UQ code UNICORN. The transient process is defined as the insertion and withdraw of the bank 1. From the numerical results, it can be found that during the transient process, the maximum relative uncertainty for the normalized assembly powers can be about 1.65% and the maximum relative uncertainty for the pin-wise power is about 2.71%.

ACKNOWLEDGEMENTS

This work is supported by the National Natural Science Foundation of China (Grant No. 11735011) and the Fundamental Research Funds for Central University (Grant No. xzy012019026).

REFERENCES

1. Boyarinov V., Fomichenko P., Hou J. and Ivanov K. Deterministic Time-Dependent Neutron Transport Benchmark without Spatial Homogenization (C5G7) Volume I: Kinetics Phase. 2016, NEA/NSC/DOC.
2. Wang B., Liu Z., Chen J., et al. A modified predictor-corrector quasi-static method in NECP-X for reactor transient analysis based on the 2D/1D transport method. Progress in Nuclear Energy, 2018, 108: 122-135.
3. Shen Q., Wang Y., Jabaay D., et al. Transient analysis of C5G7-TD benchmark with MPACT. Annals of Nuclear Energy, 2019, 125: 107-120
4. Ryu M., Joo G. nTRACER whole core transport solutions to C5G7-TD benchmark. 2017, M&C2017, Jeju, Korea.
5. Ogujiuba K., Hou J., and Ivanov K. Deterministic Time-Dependent Neutron Transport Benchmark without Spatial Homogenization (C5G7-TD) Volume I: Kinetic Phase Summary Report (DRAFT). 2019, NEA/NSC/DOC(2019).
6. Sui, Z., Cao, L., Wan, C., et al. Covariance-Oriented Sample Transformation: A New Sampling Method for Reactor-Physics Uncertainty Analysis[J]. Annals of Nuclear Energy, 2019, 134: 452-463.
7. Wan C., Cao L., Wu H. and Shen W. Total sensitivity and uncertainty analysis for LWR pin-cells with improved UNICORN code. Annals of Nuclear Energy, 2017, 99: 301 – 310.
8. MacFarlane R., Muri D., Boicurt R., et al. The NJOY Nuclear Data Processing System, Version 2016. Los Alamos National Laboratory, LA-UR-17-20093, 2016.
9. Chen J., Liu Z., Zhao C., et al. A new high-fidelity neutronics code NECP-X. Annals of Nuclear Energy, 2018, 116: 417-428.